Energy Confinement and Thermal Transport Characteristics of Net-Current Free Plasmas in Large Helical Device

H.Yamada 1), K.Y.Watanabe 1), K.Yamazaki 1), S.Murakami 1), S.Sakakibara 1), K.Narihara 1), K.Tanaka 1), M.Osakabe 1), K.Ida 1), N.Ashikawa 2), P.deVaries 1), M.Emoto 1), H.Funaba 1), M.Goto 1), H.Idei 1), K.Ikeda 1), S.Inagaki 1), N.Inoue 1), M.Isobe 1), S.Kado 1), O.Kaneko 1), K.Kawahata 1), K.Khlopenkov 1), A.Komori 1), S.Kubo 1), R.Kumazawa 1), S.Masuzaki 1), T.Minami 1), J.Miyazawa 1), T.Morisaki 1), S.Morita 1), S.Muto 1), T.Mutoh 1), Y.Nagayama 1), N.Nakajima 1), Y.Nakamura 1), H.Nakanishi 1), K.Nishimura 1), N.Noda 1), T.Notake 3), T.Kobuchi 2), Y.Liang 2), S.Ohdachi 1), N.Ohyabu 1), Y.Oka 1), T.Ozaki 1), R.O.Pavlichenko 1), B.J.Peterson 1), G.Rewoldt 4), A.Sagara 1), K.Saito 3), R.Sakamoto 1), H.Sasao 2), M.Sasao 1), K.Sato 1), M.Sato 1), T.Seki 1), T.Shimozuma 1), M.Shoji 1), H.Sugama 1), H.Suzuki 1), M.Takechi 1), Y.Takeiri 1), N.Tamura 2), K.Toi 1), T.Tokuzawa 1), Y.Torii 3) K.Tsumori 1), I.Yamada 1), S.Yamaguchi 1), S.Yamamoto 3), M.Yokoyama 1), Y.Yoshimura 1), T.Watari 1), K.Itoh 1), K.Matsuoka 1), K.Ohkubo 1), I.Ohtake 1), S.Satoh 1), T.Satow 1), S.Sudo 1), S.Tanahashi 1), T.Uda 1), Y.Hamada 1), O.Motojima 1), M.Fujiwara 1)

1) National Institute for Fusion Science, Toki, Japan
2) Department of Fusion Science, Graduate Univ. for Advanced Studies, Hayama, Japan
3) Department of Energy Engineering and Science, Nagoya University, Japan
4) Princeton Plasma Physics Laboratory, Princeton Univ. Princeton, USA

e-mail contact of main author : hyamada@lhd.nifs.ac.jp

Abstract. The energy confinement and thermal transport characteristics of net-current free plasmas in the much smaller gyro-radii and collisionality regimes than before have been investigated in the Large Helical Device (LHD). The inward shifted configuration that is superior from the theoretical aspect of neoclassical transport has revealed a systematic confinement improvement on a standard configuration. The improvement of energy confinement times on the international stellarator scaling 95 occurs with a factor of 1.6 ± 0.2 for an inward shifted configuration. This enhancement is primarily due to the broad temperature profile with a high edge value. A simple dimensional analysis involving LHD and other medium sized heliotrons yields strongly gyro-Bohm dependence ($\tau_E \Omega \propto \rho^{*-3.8}$) of energy confinement times. It should be noted that this result is attributed to comprehensive treatment of LHD for systematic confinement enhancement and that the medium sized heliotrons have narrow temperature profiles. The core stored energy still indicates the dependence of $\tau_E \Omega \propto \rho^{*-2.6}$ when data only from LHD is processed. The local heat transport analysis of dimensionally similar discharges except for ρ^* suggests that the heat conduction coefficient lies between Bohm and gyro-Bohm in the core and changes towards strong gyro-Bohm in the peripheral region. Since the inward shifted configuration has a geometrical feature suppressing the neoclassical transport, confinement improvement can be maintained in the collisionless regime where the ripple transport is important. The stiffness of the pressure profile coincides with enhanced transport in the peaked density profile obtained by pellet injection.

1. Introduction

Clarification of transport mechanisms of high temperature plasmas in magnetic fusion devices is worth challenging as a scientific issue and prerequisite for engineering design of fusion reactors. The dimensional approach is a strong method to investigate the nature of a complex system [1]. In fusion plasmas, the dimensionless parameters; i.e., normalized gyro radius ρ^*, beta value β, and collisionality ν^* are typical key parameters in determining the transport processes. In particular, careful examination by means of a wide-range scan in ρ^* is prerequisite for the establishment of a reliable scaling law since the dependence on ρ^* has a great impact on extrapolation to reactor-grade plasmas. ρ^* is also connected with the

characteristic scale length of a predominant instability; therefore, it is attracting interest in the clarification of the physical mechanism of anomalous transport. ν^* is a major parameter in helical systems since the neoclassical transport due to helical ripples is enhanced as $\propto \varepsilon_h^{3/2} T^{7/2}$, where ε_h is the helical ripple, in a low collisionality regime. The past study of medium-sized helical devices has suggested the international stellarator scaling 95 (ISS95) [2] expressed in

$$\tau_E = 0.079\, a^{2.21} R^{0.65} P_{abs}^{-0.59} \bar{n}_e^{0.51} B^{0.83} \iota_{2/3}^{0.4} \quad ,$$

with P_{abs} in MW and $\bar{n}_e$ in 10^{19}m^{-3} units, respectively, and $\iota_{2/3}$ is the rotational transform at the two-thirds radius. This scaling law can be rewritten into the non-dimensional expression

$$\tau_E \Omega \propto \rho^{*-2.71}\, \nu^{*-0.04}\, \beta^{-0.16} \quad ,$$

which indicates that the energy confinement is weak gyro-Bohm. Here Ω is the ion gyro-frequency. The investigation of transport characteristics in net-current free plasmas in extended regimes in both ρ^* and ν^* is possible in the Large Helical Device (LHD) [3].

LHD is a large superconducting heliotron with a nominal major radius R of 3.9 m, a minor radius a of 0.6 m, and magnetic field B close to 3 T. The large dimensions and strong magnetic field have extended the physical parameter envelopes in non-dimensional parameters as well as in absolute values. Parameter regimes studied here cover B of 0.75-2.9 T, line averaged densities $\bar{n}_e$ of $0.8–7.0\times10^{19}$ m^{-3} and heating power of NBI P_{abs} of 0.5-4.2 MW. These ranges of parameters can be rewritten in the non-dimensional parameters, i.e., $1.4\times10^{-3} \le \rho^* \le 5.7\times10^{-3}$, $3.0\times10^{-2} \le \nu^* \le 7.8$, $7.9\times10^{-4} \le \beta \le 2.0\times10^{-2}$. Compared with the database of medium-sized helical experiments [2], ρ^* and ν^* in LHD plasmas are reduced by half and by one order of magnitude, respectively. Here ν^* is the electron collisionality defined by $\nu^* = \sqrt{2} R q \nu_{ei} / v_{th}^e \varepsilon^{1.5}$ and the ion collisionality is similar to this since generally $T_e \sim T_i$. While the ISS95 scaling is derived from collisional plasmas ($\nu^* \ge 1$), a systematic exploration in the collisionless regime ($\nu^* < 1$) in LHD is of much importance to investigate neoclassical effect.

The present study is focused on the NBI heated plasmas which realize quasi-steady states with the condition $dW/dt \sim 0$. Since the energy of NBI (120 -160 keV) is much higher than the electron temperature (up to 3.5keV), about 80 % of the power is deposited in electrons. Power deposition is calculated by Monte-Carlo simulation in 3-D in real space and 2-D in velocity space [4]. Since the electron conduction is a primary loss channel, the electron heat transport is highlighted in the local transport analysis.

The previous study on energy confinement times [5] covers the data only from the standard configuration which is characterized by a magnetic axis position R_{ax} of 3.75 m. This geometry is selected from the balanced theoretical optimization of MHD stability and particle orbits leading to good neoclassical transport [6]. The inward shifted configuration with R_{ax} = 3.6 m has much more favorable particle orbits and mitigates the neoclassical helical ripple transport by a multi-helicity effect while the interchange instability should be of concern. The observed better performance of confinement in the case of R_{ax} = 3.6 m is described and discussed in this article.

2. Energy Confinement Time

Figure 1(a) shows the comparison of the energy confinement times obtained in the experiments with the prediction from ISS95. Tokamak data are selected from the ELMy H-mode ITER database [7]. Toroidal plasma currents are translated to rotational transform with the assumption of a safety factor q profile of $q=1+(q_a-1)\rho^4$. Since ISS95 has a similar expression to the ITER ELMy H-mode scaling, the tokamak data as well as the stellarator data scale together well. LHD plasmas stand comparison with the ELMy H-mode in large

tokamaks in general, although it should be noted that the heating power may be insufficient for a direct comparison. Enhancement for the inward shifted case with R_{ax} = 3.6 m can be seen in Fig.1(a). The distributions of enhancement τ_E/τ_E^{ISS95} have the mean values of 1.08 and 1.59 with the standard deviations of 0.14 and 0.20 for the cases of R_{ax} = 3.75 m and R_{ax} = 3.6 m, respectively. The peak of the distribution inclines to a higher value with a skewness of -0.37 in the case of R_{ax} = 3.6 m while it inclines to a lower value with a skewness of 0.23 in the case of R_{ax} = 3.75 m. When the LHD data is compared with the medium-sized heliotron/torsatrons (Heliotron E, ATF, and CHS) because of a common fundamental physics basis, the systematic enhancement can be explained by the contribution of the pedestal part [5,8] which is defined by the knee position of ρ = 0.9. Since the scale length of pedestal structure has not been clarified yet, the position of ρ = 0.9 is an expedient. The total stored energy is decomposed into the core and the pedestal parts in the following [9].

$$W = W_{core} + W_{ped}\text{, where } W_{core} = \int_{\rho=0}^{\rho=0.9} (p(\rho) - p(0.9))dV\,.$$

The core confinement can be scaled with the common weak gyro-Bohm characteristics relevant to the case of R_{ax} = 3.75 m [5] and the medium-sized heliotron/torsatrons. However the hypothesis that W_{ped} is small or negligible in the medium sized heliotron/torsatrons and that the core parts have common characteristics cannot explain the further improvement in the inward shifted configuration. The improvement of the factor of 1.6 is not only due to the high edge temperature and there exists an additional mechanism for the core confinement improvement in the inward shifted configuration.

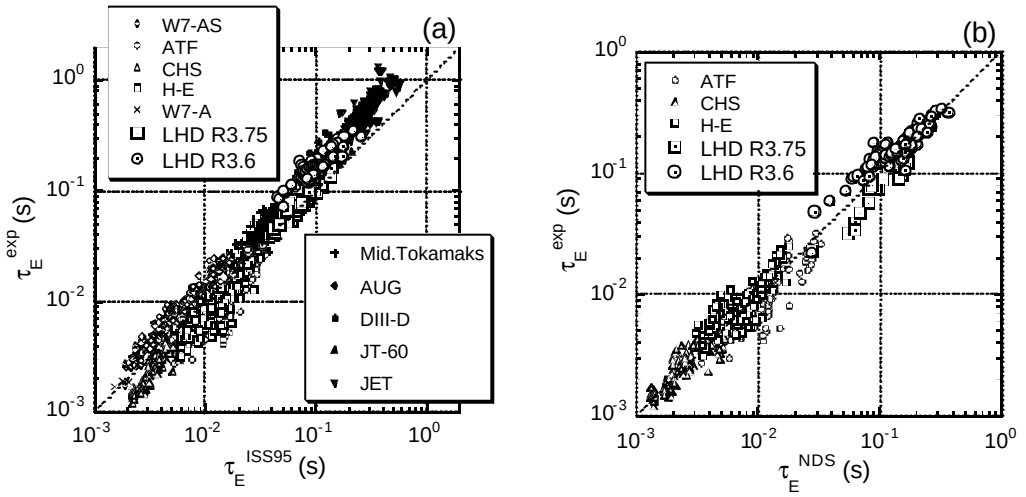

FIG.1 Comparison of the energy confinement times in the experiments with the scalings. (a) ISS95, together with tokamak ELMy H-mode data. (b)Regression analysis with non-dimensional parameters for the heliotron/torsatrons.

A simple regression analysis using non-dimensional parameters has been applied with the form $\tau_E\Omega$ = CF(ρ^*,ν^*,β,ε). Figure 1(b) shows the comparison of the experimental values with the scaling derived from this analysis for the data from heliotron/torsatrons (Heliotron E, ATF, CHS, and LHD). Here the obtained scaling is expressed as $\tau_E^{NDS}\Omega \propto \rho^{*-3.79}\,\nu^{*-0.29}\,\beta^{0.26}\varepsilon^{0.09}$ indicating a strong gyro-Bohm dependence. Combined scaling of LHD, with a significant improvement due to the pedestal parts and small ρ^*, and the medium sized heliotrons, with no significant pedestal-like feature, consequently leads to a strong gyro-Bohm expression. It should be noted that this comprehensive result does not claim that the predominant transport process in heliotron/torsatron plasmas has a strong gyro-Bohm nature. The core confinement in LHD alone has still indicated the dependence $\tau_E\Omega \propto \rho^{*-2.6\pm0.1}$

3. Investigation of Dimensionally Similar Discharges

3.1 Comparison of Dimensionally Similar Discharges with Different r*.

Comparison of dimensionally similar discharges has been widely applied in many experiments to clarify the ρ* dependence [10-13]. Two discharges with different magnetic field 2.75 T and 1.52 T are compared here. The magnetic axis is set at R_{ax}=3.6m for both cases. The density and heating power are controlled to get plasmas with the collisionality ν* and beta similar to each other. Also the Bohm term *T/B* should be close. Remarkable agreement in ν* and difference in ρ* are seen in Fig.2(c). Difference in β (0.34 % and 0.39% in the cases of 2.75 T and 1.52 T, respectively) is tolerable since β should not play an essential role [14]. The ρ* dependence is discussed for the formula; $\chi = \chi_B \rho^{*\alpha}\, F(\nu^*, \beta, q, \varepsilon, \text{etc})$. Although the safety factor *q*, or its reciprocal, the rotational transform should be important, a helical system has a great advantage to tokamaks in settting the identical condition regarding *q*. In this comparison, the function F is considered to be the same for both discharges.

Figure 2(d) shows the ratio of the electron heat conduction coefficients χ_e. The predictions from the Bohm (α=0), the gyro-Bohm (α=1), and the neoclassical calculations [15] are also illustrated. When ν* is the same, the neoclassical dependence is very close to gyro-Bohm for ν*<1. Experimental observation shows that the transport lies near gyro-Bohm for ρ<0.6 and shifts between Bohm and gyro-Bohm for 0.6<ρ<0.8. The peripheral region ρ>0.85 is found to be anomalous and strongly gyro-Bohm. The increase in the predictions from Bohm and gyro-Bohm in the peripheral region is due to the fact that the edge temperature increases more rapidly than $B^{4/3}$.

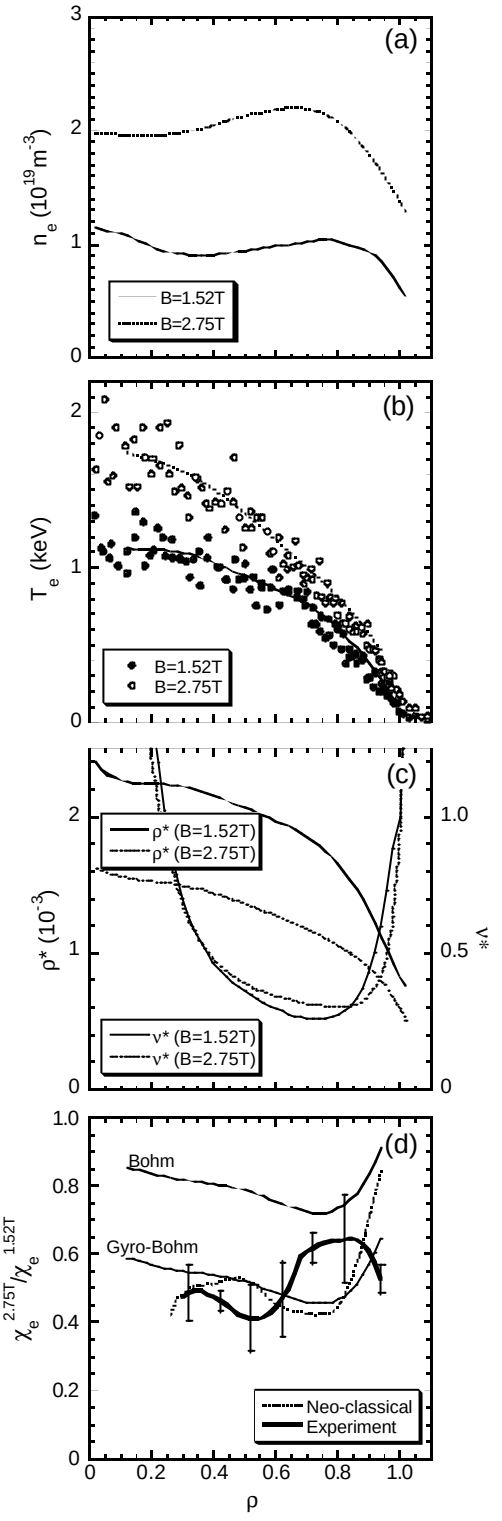

FIG.2 Dimensionally similar discharge with the different magnetic field (1.52T and 2.75T). (a) Density. (b) Electron temperature. (c) r and n*.(c)Ratio of the electron heat conduction coefficients.*

Regression analysis of the local heat transport coefficient χ_{eff} has been performed with the dimensionless parameters for 57 discharges. Figure 3 shows the profiles of the exponents of dimensionless parameters. The transport lies between Bohm and gyro-Bohm in the core, and shows a strong gyro-Bohm nature in the peripheral region. This analysis supports the above discussion of the dimensionally similar discharges.

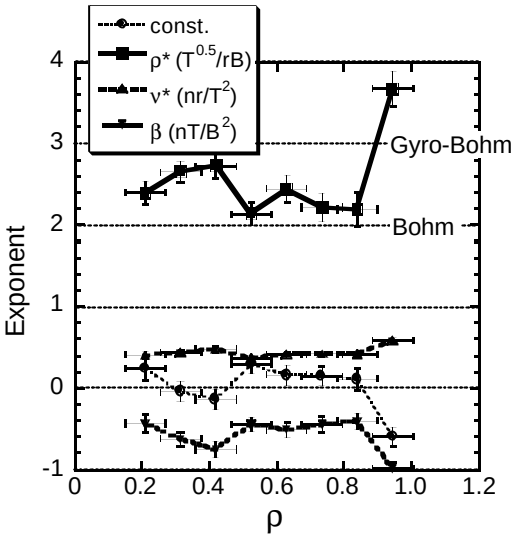

FIG 3.Profiles of exponents of dimensionless $c_{eff}/(Br^2)$ scaling.

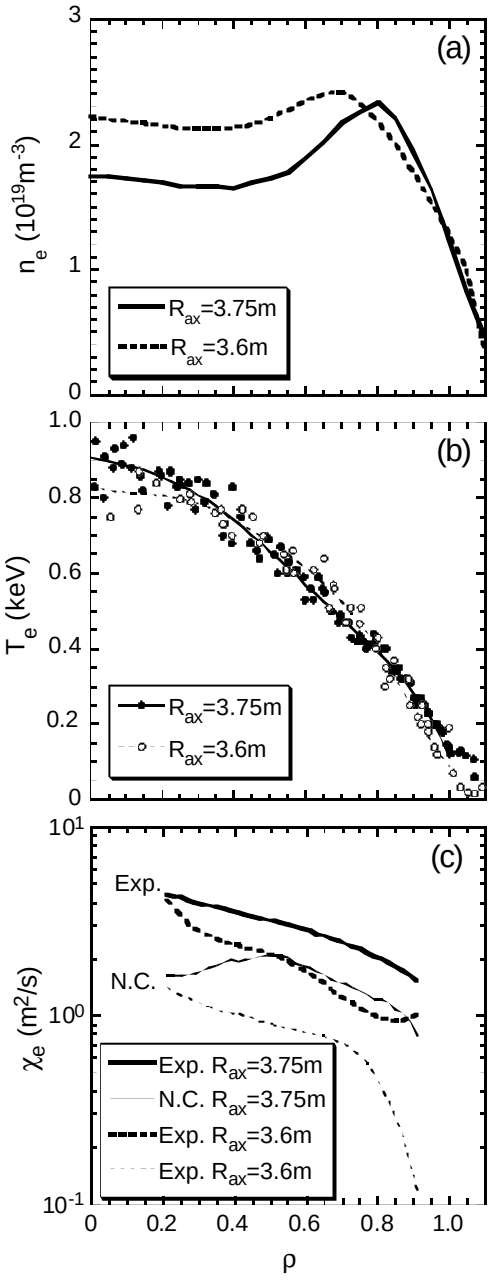

FIG.4 Profiles of (a) density, (b) temperature, and (c) electron heat conduction coefficient in dimensionally similar discharges with different magnetic axis positions.

3.2 Effect of Magnetic Axis Shift

A study on energy confinement times has indicated that the inward shift configuration (R_{ax}=3.6m) shows statistical confinement enhancement of a factor of 1.5 from the standard configuration (R_{ax}=3.75m) relative to ISS95. The reduction of neoclassical transport due the helical ripple is substantial in the inward shifted configuration. An anomalous transport model based on the self-sustained turbulence due to interchange modes also suggests that the heat conduction coefficient could be improved by 20-30% by the strong shear in the peripheral region in the case of the inward shifted configuration [16].

Figure 4 shows the temperature and density profiles and the analyzed heat conduction coefficient in the dimensionally similar plasmas with the different magnetic axis positions. The magnetic field is 1.5 T for both cases. The temperature is adjusted by the heating power for the same line-averaged density. A 60 % larger heating power is required for the standard configuration to get the same temperature as in the inward shifted configuration. Collisionality ν* is around 1 for both cases. Hollowness in the density profile is enhanced in the standard configuration, which can be related to neoclassical off-diagonal particle diffusion due to the temperature gradient [17]. Electron heat conduction is improved in the inward shifted configuration, which is consistent with the characteristics of the energy confinement time. The electron heat conduction coefficients monotonically decrease towards the edge from the core while degradation in the peripheral region has been generally observed in the

medium-sized helical experiments as well as L-mode plasmas in tokamaks. In the case of standard configuration, neoclassical transport accounts for two-thirds of the experimental value for $\rho<0.9$. Since the ripple transport is suppressed in the inward shifted configuration, the contribution of the neoclassical transport decreases to less than 50 % in the core and becomes negligible in the peripheral region. Therefore difference in the intermediate regions between two cases is partly due to the reduction of neoclassical heat flux. The superiority of the inward shifted configuration over the standard configuration can be seen in the collisional regime as well where neoclassical transport does not play an essential role; therefore, it is clear that the anomalous transport should be improved in the inward shifted configuration in addition to the neoclassical transport.

4. Profile Stiffness

Confinement improvement has been often associated with a peaked density profile. This is considered to be related to suppression of anomalous transport due to the ITG mode and to the large electric field due to the pressure gradient.

The density profile in LHD is quite flat and often accompanied by hollowness. An obvious pinch effect has not been observed in gas-fuelled discharges as it has for the medium-sized tokamaks. However, the density profiles peaks slowly on the time scale of the energy confinement time after the pellet injection [18,19], even if the pellet does not penetrate to the center.

Figure 5 shows the electron density, temperature, and pressure profile in two discharges with different fueling schemes, i.e., gas puff and pellet injection. The line averaged density and the heating power are almost the same for both cases (Gas-fueled discharge: $\bar{n}_e = 3.7 \times 10^{19}\mathrm{m}^{-3}$, P_{abs}=1.2 MW, Pellet-fueled discharge: $\bar{n}_e = 3.8\times 10^{19}\mathrm{m}^{-3}$, P_{abs}=1.1 MW). Resultant energy confinement times are 0.32 s and 0.34 s for the gas-fueled and pellet-fueled discharges, respectively. Therefore these two discharges are equivalent in global characteristics. However, the internal structures are different as seen in Fig.5. The density in the gas-fueled discharge is flat as typically seen in the LHD experiment while a peaked density profile is realized in the pellet-fueled discharge. The case of temperature is in striking contrast. The temperature profile is flattened in the core region in the case of the peaked density profile. Consequently, the electron pressure profiles become similar to each other (see Fig.5(c)).

Since the power deposition of NBI is peaked in the case of the peaked density profile (see Fig.6(a)), the flattening of the temperature profile is in the opposite direction. A significant degradation of the

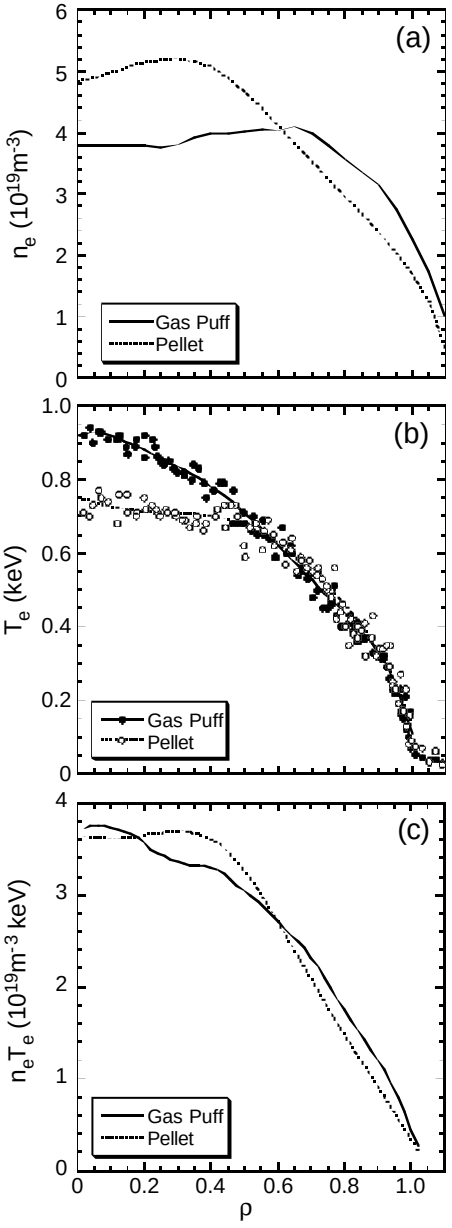

FIG.5 Profiles of (a) electron density, (b) temperature, and (c) pressure in the gas-fueled discharge (solid lines) and the pellet-fueled discharge (dotted lines).

electron heat conduction coefficient is found in the core region (see Fig.6(b)). The characteristics in the region outside the two-thirds radius are almost the same for both cases.

Enhancement of anomalous transport coincides with stiffness of the pressure profile. This feature has the trend in an other way of a typical anomalous transport candidate, the ITG mode.

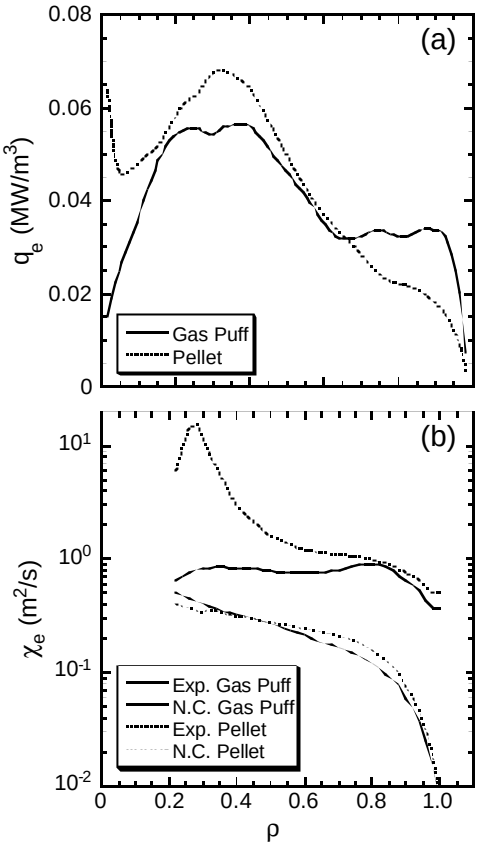

FIG.6 (a) Power deposition and (b) electron heat conduction coefficient profiles in two plasmas with gas-puff (solid lines) and pellet injection (dotted lines).

5. Discussion and Summary

As suggested in the comparison of dimensional similar discharges, the core transport in LHD has a weak gyro-Bohm nature. The characteristic change from weak gyro-Bohm to strong gyro- Bohm in the edge region (ρ>0.85) is found, which indicates a change of predominant transport mechanism. Although a drastic change in the heat conduction coefficient in the edge region has not been found yet, the profile of the heat conduction coefficient monotonically decreases towards the edge. This leads to a broad temperature profile with a high edge temperature and often appears to be an edge pedestal. Observed confinement improvement over ISS95 is primarily attributed to the large pressure at the edge. The inward shifted configuration with R_{ax}=3.6 m has characteristics of better neoclassical transport and worse MHD stability than the standard configuration with R_{ax}=3.75 m from the theoretical point of view. In the present experimental conditions, MHD instability does not degrade the global confinement up to β of 2 % [14] and further improvement has been realized in the inward shifted configuration. This improvement occurs in both the core and the edge. Plasmas with $\bar{n}_e \geq 1\times10^{19}$m^{-3} which are the subject of this study are generally collisional in the edge region, and the anomaly over the neoclassical transport is predominant there. The suppression of microturbulence due to interchange modes by the larger shear explains the improvement in the edge region by the inward shift qualitatively [16].

In the collisionless regime, the improvement in the core transport due to the reduced neoclassical ripple transport is visible in the inward shifted configuration. However, it should be pointed out that the superiority of the inward shifted configuration is maintained for ν^*>1 and the improvement is robust for collisionality. The upper envelope of confinement enhancement factor τ_E/τ_E^{ISS95} in the case of R_{ax} = 3.75 m tends to decrease like $\nu^{*-0.13}$ and no case with the enhancement factor larger than one has been observed for ν^*<0.5. The dependence of the energy confinement in the case of R_{ax} = 3.75 m shows a stronger density dependence $\tau_E \propto \bar{n}_e^{0.73}$ than in ISS95. This exponent increases from 0.7 to 0.93 when the parameter regions for ν^*>1 and ν^*<1 are considered independently. Although heat transport is substantially combination of anomalous and neoclassical transport due to toroidicity and helical ripples, these confinement characteristics in the case of R_{ax} = 3.75 m suggest that the

neoclassical ripple transport affects the upper limit of confinement in this case. The case of R_{ax}=3.6 m does not show a clear dependence on ν^*. Therefore the neoclassical ripple loss does not limit the performance in the inward shifted configuration in the current condition. Although a ripple transport is enhanced with proportion to $T_e^{7/2}$, it would not be serious in the higher temperature (> 4 keV) plasmas in future experiment with the higher heating power if help by the electric field is expected through the transition to the electron root [20,21]. It should be noted that all plasmas included in this study are in the ion-root condition.

Although the ITG and TEM modes are major candidates for anomalous transport, preliminary results suggest that both modes are stable in the core region (ρ<0.8) in both the standard and inward-shifted configurations from a linear kinetic microinstability calculation [22]. This feature is analogous to stabilization of the ITG mode in a reversed shear configuration in tokamaks. The structure of the helical ripples together with the negative magnetic shear can stabilize the ITG mode through shortening the connection length between adjacent good and bad curvature regions and reducing the bad curvature region on the outside of the torus [23]. Together with an explanation of the stiffness of the pressure profile coinciding with enhanced transport for peaked density profiles, clarification of anomalous transport in the core region, in particular improvement in the case of R_{ax} = 3.75 m, in LHD awaits solution.

Acknowledgements

The authors are grateful to all members of the device engineering group for their operational support. The continuous encouragement of ex-Director General A.Iiyoshi is gratefully acknowledged. Dr.T.Takizuka and Dr.Y.Miura kindly made the ITER database available to the authors.

References

[1] KADOMTSEV,B.B., Sov. Phys. J. Plasma Phys. **1** (1975) 295.
[2] STROTH, U., et al., Nucl. Fusion **36** (1996)1063.
[3] IIYOSHI, A., et al., Nucl. Fusion **39** (1999) 1245.
[4] MURAKAMI, S., et al., Trans.Fusion Technol. **27** (1995) 256.
[5] YAMADA, H., et al., Phys.Rev.Lett. **84** (2000)1216.
[6] OKAMOTO, M., et al., Plasma Phys. Control. Fusion **41** (1999) A267.
[7] ITER PHYSICS EXPERT GROUPS ON CONFINEMENT AND TRANSPORT AND CONFINEMENT MODELLING AND DATABASE, ITER PHYSICS BASIS EDITORS, Nucl. Fusion **39** (1999) 2175.
[8] OHYABU, N., et al., Phys.Rev.Lett. **84** (2000)103.
[9] CORDEY, J.G., et al., Nucl. Fusion **39** (1999) 301.
[10] HAWRYLUK, R.J., et al., Plasma Phys. Control. Fusion **33** (1991) 1509.
[11] WALTZ, R.E., et al., Nucl. Fusion **32** (1992) 1051.
[12] CHRISTIANSEN, J.P., Plasma Phys. Control. Fusion **34** (1992) 1881.
[13] STROTH, U., et al., Phys. Rev. Lett. **70** (1993) 936.
[14] SAKAKIBARA, S., et al., EXP3/12 in this conference.
[15] YAMAZAKI, K. and AMANO, T., Nucl. Fusion **32** (1992) 633.
[16] ITOH, K., et al., Plasma Phys. Control. Fusion **36** (1994) 1501.
[17] MAASSBERG, H., et al, Plasma Phys. Control. Fusion **41** (1998) 1135.
[18] YAMADA, H., et al., to be published in Fusion Engr./Design.
[19] SAKAMOTO, R., et al., EXP4/18 in this conference.
[20] KICK,M.,et al., Plasma Phys. Control. Fusion **41** (1999) A549.
[21] IDA, K., et al., EX9/4 in this conference
[22] REWOLDT, G., et al., to be published in Phys. Plasmas.
[23] KURODA, T. et al., J.Phys.Soc.Japan **67** (1998) 3787.